Diversity driven unbiased search of minimum energy cluster configurations

2009 J. Phys.: Condens. Matter 21 084209

(http://iopscience.iop.org/0953-8984/21/8/084209)

J. Phys.: Condens. Matter **21** (2009) 084209 (10pp) doi:10.1088/0953-8984/21/8/084209

Diversity driven unbiased search of minimum energy cluster configurations

José Rogan[1], Max Ramírez[1], Víctor Muñoz[1], Juan Alejandro Valdivia[1], Griselda García[2], Ricardo Ramírez[2] and Miguel Kiwi[1,2]

[1] Departamento de Física, Facultad de Ciencias, Universidad de Chile, Casilla 653, Santiago, Chile
[2] Facultad de Física, Universidad Católica de Chile, Casilla 306, Santiago, Chile

E-mail: jrogan@macul.ciencias.uchile.cl

Received 8 July 2008, in final form 19 August 2008
Published 30 January 2009
Online at stacks.iop.org/JPhysCM/21/084209

Abstract

The determination of the spatial distributions that atoms adopt to form condensed matter is a problem of crucial importance, since most physical properties depend on the atomic arrangement. This is especially relevant for clusters, where periodicity is nonexistent. Several optimization procedures have been implemented to tackle this problem, with ever increasing success. Here we put forward a search scheme which preserves as large a diversity as allowed by the use of phenomenological potentials, generating in an unbiased fashion a bank of configurations to be explored; a procedure we denominate diversity driven unbiased search (DDUS). It consists in the generation, using phenomenological potentials, of a data bank of putative minima rather than a single, or just a few, configurations which are based on the conformational space annealing method (CSA). All of the configurations in the bank are thereafter refined by means of DFT computations. Certainly, in spite of our efforts to generate a bank as diverse as possible, not all relevant structures might be included in it, since quantum effects are ignored. The procedure is applied to several examples of rhodium, palladium, silver, platinum and gold clusters, between 5 and 23 atoms in size. The main conclusion we reach is that unbiased search, among a significant number of candidates, quite often leads to rather unexpectedly low symmetry configurations, which turn out to be the lowest energy ones within our scheme.

(Some figures in this article are in colour only in the electronic version)

1. Introduction

Nanoclusters have attracted the interest of physicists, chemists and applied scientists, due to their challenges to basic science and because of the variety of potential and actual technological uses they have [1]. From a basic science point of view they constitute a natural bridge between the macroscopic bulk limit and the microscopic scale of atoms and molecules. On the application side they have found a large variety of uses in technologies that span the range from catalytic processes, hydrogen conversion, increasing the octane grade of gasolines all the way to optoelectronics.

But, as Goedecker *et al* [2] recently pointed out, the first and most fundamental step in the description and understanding of clusters is the precise determination of the geometrical configuration that the constituent atoms adopt, since most physical properties depend on the structure of the system. This has generated significant interest and activity in the field.

However, the complexity of the problem is quite overwhelming, as can easily be perceived by pointing out that a 13 atom cluster, interacting via a Lennard-Jones two-body potential, has a potential energy surface function with around 1000 minima. Even more impressive is that for a 147 atom cluster this number grows to $\sim 10^{50}$ minima [3].

Thus, recently the search for minimum energy cluster configurations has received much attention, which has led to the development of several strategies to obtain them [4–9].

Certainly, the ideal procedure would be to implement an unbiased search using exclusively *ab initio* or density functional theory (DFT) codes; however, at present such an approach is out of the question, especially for larger clusters, because of the extremely long number crunching times that would be required. Thus, the strategies put forward differ in the accuracy they pretend to achieve. Obviously, increasing accuracy has a steep cost in computer resources.

Among the strategies that have been developed we can distinguish at least four categories:

(i) To simply use two body [3, 5, 10, 11] or more refined phenomenological potentials [12–14] and global optimization techniques to obtain, fairly quickly, rough estimates of the minimum energy of the cluster configuration. This approach is at present the only feasible one to explore very large clusters [15, 16].
(ii) To use less expensive quantum methods, such as tight binding, to compute structural [17] and even magnetic properties [18–21] of larger clusters ($N > 100$).
(iii) To adopt a set of high symmetry structures and refine them *ab initio* keeping the original symmetry fixed. For example, Yang *et al* [22, 23] investigated, exploring an extensive structural database plus DFT refinement, the configurations of Cu_n clusters, for $8 \leqslant n \leqslant 20$, and Ag clusters, for $9 \leqslant n \leqslant 20$.
(iv) To allow for arbitrary symmetry when implementing the *ab initio* refinement [24–27].

Using the latter approaches it becomes apparent that the minimum energy cluster structure obtained with phenomenological potentials does not necessarily converge to the one with the lowest energy after DFT refinement [27]. Actually, this is the main point we want to convey with the present paper: it is extremely unlikely that simple inspection of the set of minima obtained by means of phenomenological potentials can give clues to which one of them is the best candidate for the global minimum. Our conclusion is that a large set of candidates has to be re-optimized with DFT techniques to improve the probability of actually being able to find the global minimum.

Thus, given the fact that the potential energy surface is so complex and that it has such a large number of minima, the preservation of diversity of the candidates for DFT refinement is of central importance. Failing to preserve the diversity of the candidates for DFT refinement strongly increases the probability of missing low lying energy configurations. Thus, unbiased search strategies, based on phenomenological potentials, are the most suitable ones, at the price of an additional computational effort. In this contribution we present a successful unbiased search strategy which, implemented with the aim of keeping as large a diversity as feasible, combines the use of many-body phenomenological potentials with DFT refinement. We call this procedure diversity driven unbiased search (DDUS). More precisely the procedure incorporates all of the following elements: the creation of a data bank with a fixed number of configurations N_b using CSA [28–30] with phenomenological potentials to ensure diversity, followed by DFT re-optimization.

Certainly, the interesting and important generalization of these techniques to the study of binary clusters is considerably more challenging and complex. However, significant progress has recently been achieved in this most promising new field [26, 31–33].

This paper is organized as follows. After this introduction, in section 2 we present the basic ideas used to generate the data banks. In section 3 we describe the many-body phenomenological potential we use. The cluster structure classification is discussed, on the basis of a 'distance' among the several configurations, in section 4, where a comparison between several options for the concept of distance between configurations is also given, and a simple and convenient alternative definition is suggested. The codification of a particular structure, and the genetic operations employed to generate it, are described in section 5. In section 6 we provide the technical details of the strategy we implemented and the codes we used. In section 7 the results obtained with our procedure, as applied to several illustrative examples, are given. Finally, section 8 closes the paper with an analysis of the method and a discussion of the results that were obtained.

2. Generation of the data bank

A novel and powerful global optimization method, based on evolutionary type algorithms and called conformational space annealing (CSA), was put forward by Lee, Scheraga *et al* [28–30] and applied extensively by them to the protein folding problem [29, 30] and, more recently, to the global optimization of Lennard-Jones clusters [34]. The key feature that makes CSA advantageous is the fact that it yields a data bank of low lying minima, while at the same time it preserves diversity. As a comparison, the more standard genetic algorithm (GA) methods, due to their notable efficiency, have a tendency to collapse most of the initial populations into a single global minimum, eliminating most of the diversity in the solutions.

CSA starts with a set of configurations, denominated *the bank*. In our implementation we have used banks of $N_b = 15$, 30, and 50 different configurations for clusters of $N = 5$, 13, and 23 atoms, respectively. For the clusters in the initial bank, each of the three atomic coordinates of each atom are chosen at random within the range $\{0, N^{1.32}\}$ [Å], where N is the number of atoms in the cluster. The exponent 1.32 is adopted on the basis of an empirical best fit, intended to achieve maximum diversity. These N_b configurations are locally minimized, using the many-body phenomenological potential specified in section 3, with the quasi-Newton L-BFGS routine [35] and a modified steepest descent method to manage compressed and distended situations. Among the resulting configurations, 40% are chosen at random as seeds to generate new configurations. Each seed is used to generate a population of $N_p = 0.6 \times N_b$ new configurations through the genetic operations that will be described below in section 5: two thirds by mating with another configuration chosen from the bank, and one third by mutation. All the new configurations in these populations are locally minimized. From this locally optimized population, the ith configuration is incorporated into the bank if it satisfies one of the following conditions: (i) if the distance $D(i, k_{min})$, which

is defined in section 4, between the ith configuration and the closest configuration $k_{\min}$ in the bank is small ($< D_{\text{cut}}$), then the configuration with the largest energy of the two is replaced by the other one; (ii) if the distance $D(i, k_{\min})$ between the ith configuration and the closest configuration $k_{\min}$ in the bank is large ($> D_{\text{cut}}$) then the largest energy configuration in the bank is removed. The threshold distance D_{cut} is chosen as the average pair distance among all the configurations considered in the initial optimized bank. This way the diversity is improved as the bank is constantly being renewed, and we choose to stop this renewal when all the bank members have been used as seeds. This process has been defined as an iteration in the original CSA method. We chose to apply three iterations starting from the final bank of the previous iteration, while keeping D_{cut} fixed.

3. Many-body potentials

We now outline key features related to the phenomenological potentials we used in our calculations. At the outset one might think that elementary pair potentials should be sufficient to achieve the task. However, metals are not properly described by pair potentials since they are not capable of reproducing, for example, many of the dynamical properties of the material nor the so-called Cauchy discrepancy, which the elastic constants of most cubic crystals satisfy: i.e. $c_{11} \neq c_{44}$. Another serious drawback of the use of pair potentials is the incorrect estimate of the vacancy formation energy, whose value turns out to be almost equal to the cohesive energy (E_{b}), whereas experimental results [36] indicate that they range around $E_{\text{b}}/3$. Moreover, as pointed out by Ferrando *et al* [37], the many-body character of the interaction potential must account for bond order/bond length correlation, which is a many-body effect. However, empirical potentials leave out quantum effects, such as shell closure and quantum interference.

The many-body embedded atom method (EAM) was put forward as an alternative to the use of pair potential models [12, 38]. The EAM assumes that each atom in a solid can be regarded as an impurity embedded in the host of the remaining atoms, so that the total electron density is approximated by the superposition of the electron densities of the individual atoms. Thus, the electron density in the vicinity of each atom can be written as the sum of the densities of each atom plus the electron densities from all the surrounding ones. By making the simplifying assumption that this background electron density is a constant, an embedding energy is defined as a function of the background electron density of the particular atomic species. Possibly the first successful attempt in this context is due to Daw, Foiles and Baskes [12, 38] who put forward a formalism known as the embedded atom method (EAM). This formalism was improved upon by Voter and Chen [39]. To apply this method, the embedding function, pair repulsions, and atomic densities must be known. Approximate values of the embedding functions and pair interactions can be calculated from the formal definitions of these quantities within the DFT framework. Other formalisms, different from EAM but related to it, were put forward by Ducastelle [40], Gupta [14, 36], Sutton and Chen [41] and, more recently, by Murrell and Mottram [42, 43].

Table 1. Parameters employed for the Gupta potential.

Metals	A (eV)	ξ (eV)	p	q	r_0 (Å)
Rh	0.0629	1.660	18.450	1.867	2.69
Pd	0.1746	1.718	10.867	3.742	2.75
Ag	0.1028	1.178	10.928	3.139	2.89
Pt	0.2975	2.695	10.612	4.004	2.77
Au	0.2061	1.790	10.229	4.036	2.88

We chose the Gupta potential [36] for the rest of this paper, because it has a very simple analytical form which depends on five parameters. It was derived from Gupta's expression for the cohesive energy E_{b} of the bulk material [14] and is based on the second moment approximation to tight binding theory. It is written in terms of a repulsive pair potential and an attractive many-body term. The attractive many-body term (the band energy) for the ith atom is given by

$$E_{\text{b}}^i = -\left[\sum_j \xi^2 \exp\left\{-2q\left(\frac{r_{ij}}{r_0} - 1\right)\right\}\right]^{1/2}. \tag{1}$$

The stability of the system is ensured by adding a phenomenological core-repulsion term of the Born–Mayer type, which for a pure element reads

$$E_{\text{r}}^i = A\sum_j \exp\left[-p\left(\frac{r_{ij}}{r_0} - 1\right)\right]. \tag{2}$$

In these expressions r_{ij} is the distance between atoms i and j, r_0 is the bulk first neighbor distance. A, ξ, p, and q are parameters fitted to bulk properties of the specific metal, i.e., the cohesive energy, the bulk modulus, and the cancelation of the energy gradient at r_0. Moreover, the cohesive energy of the system is given by

$$E_{\text{c}} = \sum_i (E_{\text{b}}^i + E_{\text{r}}^i). \tag{3}$$

The values we adopted for the parameters were taken from Cleri and Rosato [36], and are given in table 1.

4. The concept of distance between configurations

A tricky question does arise when one tries to establish if two clusters are equal or different. Even visual inspection is not very helpful because it strongly depends on the spatial orientation of the cluster. In this context several parameters have been suggested with some degree of success. Grigoryan *et al* [44] put forward the following definition for the distance $S_{\alpha,\beta}$:

$$S_{\alpha,\beta} = \left(1 + \frac{q_{\alpha,\beta}}{u_I}\right)^{-1}, \tag{4}$$

$$q_{\alpha,\beta} = \left[\frac{2}{N(N-1)}\sum_{n=1}^{N(N-1)/2}(d_n^{(\alpha)} - d_n^{(\beta)})^2\right]^{1/2}, \tag{5}$$

where $\{d_n^{(\alpha)}\}$ is the sorted set of all $\frac{1}{2}N(N-1)$ interatomic distances of the αth configuration, and $u_I = 1$ Å.

Lee *et al* [34] introduced the distance $D(\alpha, \beta)$ we actually employed in the generation of the data banks used in our calculations. It is given by

$$D(\alpha,\beta) = \sum_m m(2|H_\alpha(1,m) - H_\beta(1,m)| + |H_\alpha(2,m) - H_\beta(2,m)|) \quad (6)$$

where $H_\alpha(1,m)$ $[H_\alpha(2,m)]$ is the histogram of the number of atoms having m neighbors in the first (second) shell of the αth configuration. To specify the shell radii we adopt the first and second neighbor distances of the respective bulk lattice, which in this particular instance is fcc. This way of specifying the distance has the obvious disadvantage that the first and second neighbor distances, unknown *a priori* are defined somewhat arbitrarily. In [27] and here we have used the bulk first and second neighbor distances for this purpose.

We propose a new definition of the distance, between configurations α and β of N atom clusters, which proved quite simple and successful. It is given by

$$d_{\alpha,\beta} = \frac{1}{N}\left|I_{\max}^{(\alpha)} - I_{\max}^{(\beta)}\right| \quad (7)$$

where α and β label specific cluster configurations and $I_{\max}^{(\alpha)}$ is the largest of the three eigenvalues of the matrix whose elements are

$$I_{ij}^{(\alpha)} = \sum_{n=1}^{N}[(r_n^{(\alpha)})^2\delta_{ij} - x_{n,i}^{(\alpha)}x_{n,j}^{(\alpha)}] \quad (8)$$

where $(r_n^{(\alpha)})^2 = \sum_{i=1}^{3}(x_{n,i}^{(\alpha)})^2$. The $x_{n,i}^{(\alpha)}$'s are the ith Cartesian coordinates of atom n measured relative to the coordinates of the cluster center of mass, for the αth configuration.

We found that this distance $d_{\alpha,\beta}$ is quite convenient to compute and very sensitive to changes in cluster topology. Moreover, since it does not require the knowledge of the cutoff radii, it is very convenient and easily implemented. In addition, by determination of the principal or singular axis of the $I_{ij}^{(\alpha)}$ matrix, the graphic representation of the cluster becomes uniquely defined, rather than depending on the angle of sight. However, the problem of defining the distance, in a convenient and universal way, is by no means a closed subject. Among other open questions the extension to binary clusters is not trivial.

5. Generating diversity

Now we describe the genetic operations used in our procedure. A configuration is specified by $3N$ real numbers, the Cartesian coordinates of the N atoms of the cluster, which we enumerate as

ζ_1	ζ_2	ζ_3	$\cdots$	ζ_{p-2}	ζ_{p-1}	ζ_p	ζ_{p+1}	ζ_{p+2}	$\cdots$	ζ_{3N-2}	ζ_{3N-1}	ζ_{3N}

Next, we define the following genetic operations:

(i) *Inversion*: We choose two random integers, such that $0 < r < p < 3N$, and relabeling our initial configuration as follows:

ζ_1	ζ_2	$\cdots$	ζ_{r-1}	ζ_r	ζ_{r+1}	$\cdots$	ζ_{p-1}	ζ_p	ζ_{p+1}	$\cdots$	ζ_{3N-1}	ζ_{3N}

we obtain, by inverting the order of all the coordinates between r and p, the new configuration

ζ_1	ζ_2	$\cdots$	ζ_{r-1}	ζ_p	ζ_{p-1}	$\cdots$	ζ_{r+1}	ζ_r	ζ_{p+1}	$\cdots$	ζ_{3N-1}	ζ_{3N}

(ii) *Coordinate replacement*: We choose a random integer, such that $0 \leqslant r \leqslant 3N$, and specify the initial configuration by

ζ_1	ζ_2	$\cdots$	$\cdots$	$\cdots$	ζ_{r-1}	ζ_r	ζ_{r+1}	$\cdots$	$\cdots$	$\cdots$	ζ_{3N-1}	ζ_{3N}

Changing ζ_r by a random number ξ_r, chosen within the same range used to construct the initial bank, one obtains

ζ_1	ζ_2	$\cdots$	$\cdots$	$\cdots$	ζ_{r-1}	ξ_r	ζ_{r+1}	$\cdots$	$\cdots$	$\cdots$	ζ_{3N-1}	ζ_{3N}

(iii) *Cluster replacement*: We write the initial configuration as

ζ_1	ζ_2	$\cdots$	ζ_{r-1}	ζ_r	ζ_{r+1}	$\cdots$	ζ_{m-1}	ζ_m	ζ_{m+1}	$\cdots$	ζ_{3N-1}	ζ_{3N}

and change every coordinate in the configuration by a random number, chosen within the same range used to construct the initial bank, to obtain

ξ_1	ξ_2	$\cdots$	ξ_{r-1}	ξ_r	ξ_{r+1}	$\cdots$	ξ_{m-1}	ξ_m	ξ_{m+1}	$\cdots$	ξ_{3N-1}	ξ_{3N}

(iv) *Arithmetic mean*: We take two initial configurations

ζ_1	ζ_2	$\cdots$	ζ_{r-1}	ζ_r	ζ_{r+1}	$\cdots$	ζ_{m-1}	ζ_m	ζ_{m+1}	$\cdots$	ζ_{3N-1}	ζ_{3N}

ξ_1	ξ_2	$\cdots$	ξ_{r-1}	ξ_r	ξ_{r+1}	$\cdots$	ξ_{m-1}	ξ_m	ξ_{m+1}	$\cdots$	ξ_{3N-1}	ξ_{3N}

that generate the descendant as follows:

κ_1	κ_2	$\cdots$	κ_{r-1}	κ_r	κ_{r+1}	$\cdots$	κ_{m-1}	κ_m	κ_{m+1}	$\cdots$	κ_{3N-1}	κ_{3N}

where

$$\kappa_i = \frac{\zeta_i + \xi_i}{2}. \quad (9)$$

(v) *Geometric mean*: We take two initial configurations

ζ_1	ζ_2	$\cdots$	ζ_{r-1}	ζ_r	ζ_{r+1}	$\cdots$	ζ_{m-1}	ζ_m	ζ_{m+1}	$\cdots$	ζ_{3N-1}	ζ_{3N}

ξ_1	ξ_2	$\cdots$	ξ_{r-1}	ξ_r	ξ_{r+1}	$\cdots$	ξ_{m-1}	ξ_m	ξ_{m+1}	$\cdots$	ξ_{3N-1}	ξ_{3N}

that generate the descendant as

κ_1	κ_2	$\cdots$	κ_{r-1}	κ_r	κ_{r+1}	$\cdots$	κ_{m-1}	κ_m	κ_{m+1}	$\cdots$	κ_{3N-1}	κ_{3N}

where

$$\kappa_i = \mathrm{sgn}(\zeta_i\xi_i)\sqrt{|\zeta_i\xi_i|}. \quad (10)$$

(vi) *Plane crossover*: Start choosing an integer $0 < i < N$. Next we take two clusters in three dimensional spatial space and rotate them, using three arbitrary Euler angles for each cluster. Next, we cut them using two $z =$ constant planes, such that both clusters are divided into two pieces with i and $N - i$ atoms. The first $3i$ elements of the configuration of the descendant correspond exactly to the i atoms of the first cluster below the first plane, and the last $3N - 3i$ elements of the configuration of the descendant corresponds exactly to the $N - i$ atoms of the second cluster that are above the second plane.

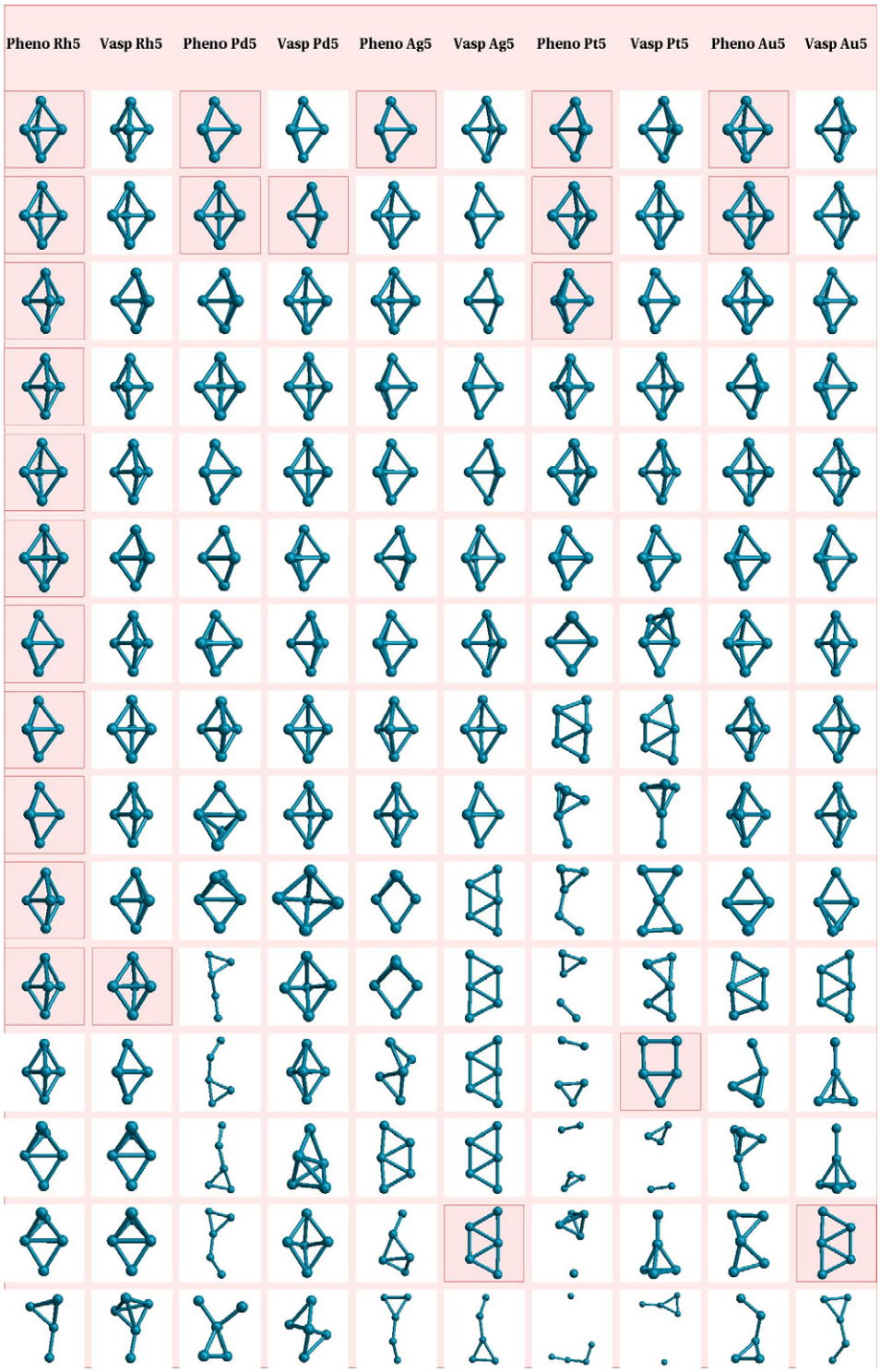

Figure 1. Illustration of the 15 structures of the 5 atom cluster banks for rhodium, palladium, silver, platinum and gold. For each one of the elements considered there are two columns; the left one (denoted by P) illustrates the DDUS bank obtained using phenomenological potentials, ordered from top to bottom by increasing energy. The right column (denoted by V) depicts the configuration after re-optimization with VASP. The structures with the gray background are the lowest energy ones (when several of them have this background they have the same energy).

6. Technical details

6.1. Minimization scheme

The procedure we implement is to close in on the minimal energy structure using phenomenological potentials and geometrical optimization via CSA, then to follow that by DFT refinement. The procedure we denominate DDUS incorporates all of the following elements: the creation of a data bank with a fixed number of configurations N_b using CSA with phenomenological potentials and genetic

operations, to ensure diversity, keeping the value of $D_{\rm cut}$ fixed. The total bank generated this way is subject to DFT re-optimization. A similar scheme has recently been put forward by Ferrando *et al* [37]. The synergy between *ab initio* and classical methods thus allows one to significantly reduce the resources that are required and to expand the set of problems amenable to treatment. In addition, the increased computational speed allows one to implement evaluation intensive minimization procedures. There are many alternative minimization methods in the literature [45–48]. For example, Sebetci and Güvenç [49] in their study of Pt, have concluded that for clusters between 22 and 56 atoms, basin hopping Monte Carlo is more efficient than molecular dynamics and thermal quenching, but that with a few exceptions the minimal structures that result are quite similar.

6.2. DFT VASP code implementation

In all the DFT calculations we used the *ab initio* VASP (Vienna *Ab initio* Simulation Package) code [50–52] with a plane-wave basis and GGA pseudopotentials, using the projector-augmented wave method (PAW) [53, 54]. The kinetic energy cutoffs used were the maximal default values recommended by the pseudopotential database, namely 250 eV. For the exchange–correlation functional we used the spin polarized generalized gradient conjugate approximation [55]. A cubic supercell with a side dimension of 20 Å was employed in the calculation. Only the Γ point was evaluated in the Brillouin zone integration, since 3 × 3 × 3 Monkhorst–Pack k-point mesh computations, where all the atoms are allowed to relax following Hellmann–Feynman forces, yield equivalent results for the total energy. The cluster geometry is optimized, without symmetry constraints, until the total energy converges to 10^{-4} eV in the self-consistency loop and the force on each atom is less than 0.05 eV Å^{-1}. The energy spread σ was set equal to 0.02 eV.

7. Results

We now present results of the implementation of our diversity driven unbiased search (DDUS) for several metal clusters. Specifically rhodium, palladium, silver, platinum and gold clusters of 5, 13 and 23 atoms. The idea is to illustrate the power of the method and to show that it leads to some novel and rather unexpected results.

First, in figure 1 we present the banks we generated on the basis of the scheme outlined in section 2 for 5 atom clusters of Rh, Pd, Ag, Pt and Au. In this 5 atom case we limited the bank to 15 specimens for each element. From top to bottom they are ordered in increasing energy as obtained with phenomenological potentials. It is apparent that the lowest energy structures obtained phenomenologically are all three dimensional, while after VASP refinement Ag_5, Pt_5 and Au_5 adopt planar configurations as the most stable ones. Moreover, they are obtained by refinement of the 14th, 12th and 14th structure, respectively, of the phenomenological data bank. It is also quite apparent that by simple inspection, and/or symmetry arguments, they would not have been the first choice

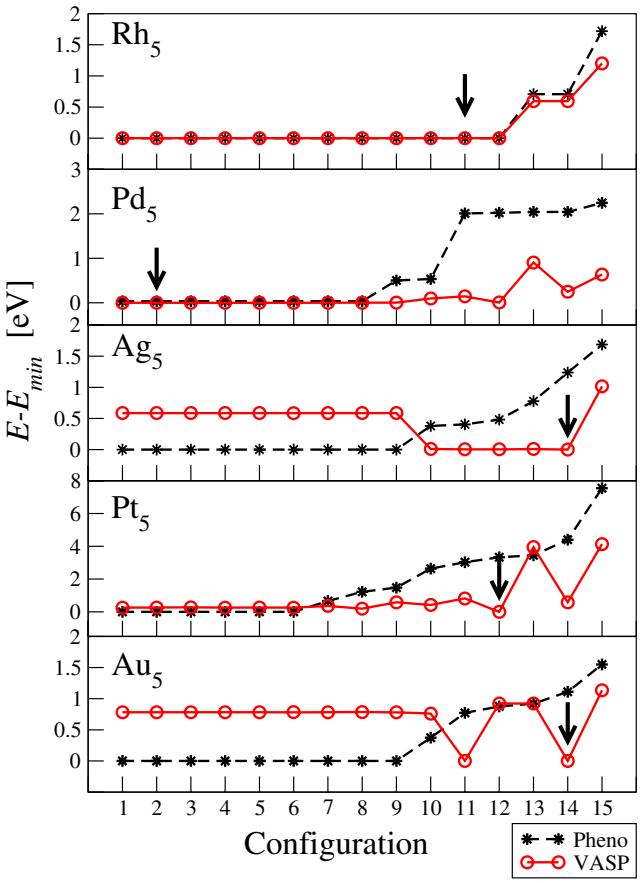

Figure 2. Energies of 5 atom clusters of rhodium, palladium, silver, platinum and gold, computed both with phenomenological potentials (stars) and after relaxation with VASP (open circles); the lines are just a guide to the eye. All energy values are referred to the minimum energy configuration. The arrows denote the specimen that attains the energy minimum after VASP relaxation.

for putative minima. In addition, the coincidence between phenomenological and DFT energy values for Rh_5 is quite remarkable, but is due to the fact that all but one of the configurations in the bank are quite similar. The values of the energies of all these clusters are displayed in figure 2. The refined lowest energy configurations are illustrated, in more detail, in figure 3.

In figure 4 we display the energies of the phenomenological and VASP refined data banks of rhodium, palladium and silver 13 atom clusters. We again observe that the refined lowest energy configurations are not the most likely *a priori* candidates. However, they are all three dimensional. Of special interest is the Pd_{13} configuration, since in a previous publication [56], using the GA and relaxing with the SIESTA code, we found the icosahedron as the lowest energy configuration. Using DDUS with VASP refinement we obtain several structures with lower energies than the Pd_{13} icosahedron, all of them less symmetrical. However, the energy reduction is slight and amounts to just ≈0.25 eV. We checked these values using VASP with both ultrasoft and PAW-GGA potentials. These results stress once again the power of an unbiased search in the quest for minimal energy configurations. The refined lowest energy configurations are illustrated in figure 5.

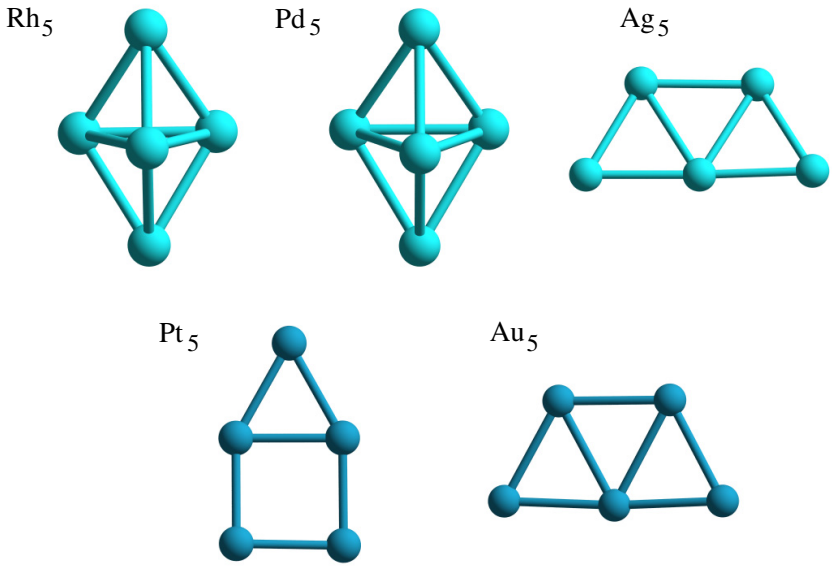

Figure 3. Geometric configuration of the 5 atom rhodium, palladium, silver, platinum and gold clusters with lowest energies as obtained with our procedure. The three latter ones are essentially planar.

In figure 6 we display the energies of the phenomenological and VASP refined data banks of palladium and silver 23 atom clusters. Once more the refined lowest energy configurations are of rather low symmetry and are illustrated in figure 7.

Several important physical characteristics of the lowest energy configurations are summarized in table 2. More precisely, the cohesion energy $E_{\rm coh}$, the average nearest neighbors distance, the cutoff radius for nearest neighbor distance as computed after refinement, the symmetry group, the fraction of cluster atoms with bulk coordination, the average coordination and the magnetic moments of all the structures illustrated in figures 3, 5 and 7 are organized in table 2. In general the lowest energy configurations are quite regular and do not display a large symmetry. The most striking deviations from average values are the large magnetic moments of Rh_{13} and Pd_{13}, of 11 and 6 Bohr magnetons, respectively. However, a word of caution should be added as to the reliability of these values, since small geometry variations imply elastic energy changes that are much larger than the magnetic energies that are involved [57]. It is also worth mentioning that none of the 5 or 13 atom clusters have fully coordinated atoms; actually, only for the 23 atom clusters do one or two atoms achieve bulk coordination.

Actually, the most striking shortcoming of the present work is the failure to obtain the lowest reported energy configuration of several small cluster structures, such as Pd_{13} and Rh_{13} [58–60]. In fact, the energy of the cubic-like structure of Rh_{13}, when calculated with the Gupta potential, lies around 10 eV above the buckled biplanar one, and is unstable. It is thus excluded from the data bank because of its large energy. Results such as these underline the main point we stress in this contribution, which is that the minima obtained phenomenologically are not necessarily good ground state candidates as computed with *ab initio* techniques. At present we are exploring several alternatives to overcome this snag in our procedure.

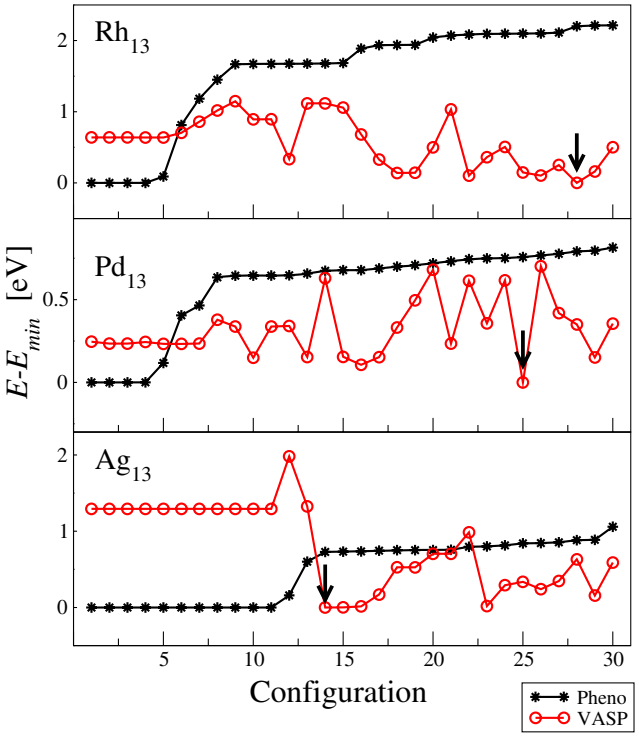

Figure 4. Energies of 13 atom clusters of rhodium, palladium and silver, computed both with phenomenological potentials (stars) and after relaxation with VASP (open circles); the lines are just a guide to the eye. All energy values are referred to the minimum energy configuration. The arrows denote specimens that attain the energy minimum after VASP relaxation.

8. Discussion and conclusions

In this contribution we have outlined and implemented an unbiased search procedure to obtain the minimum energy configurations of metallic clusters. Our purpose is to preserve

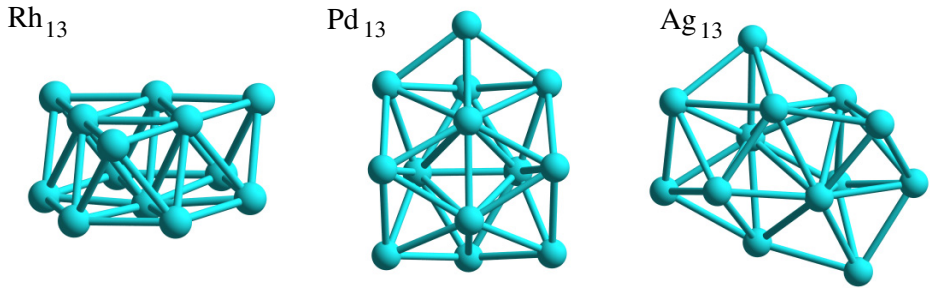

Figure 5. Geometric configuration of the 13 atom rhodium, palladium and silver clusters with lowest energies as obtained with our procedure.

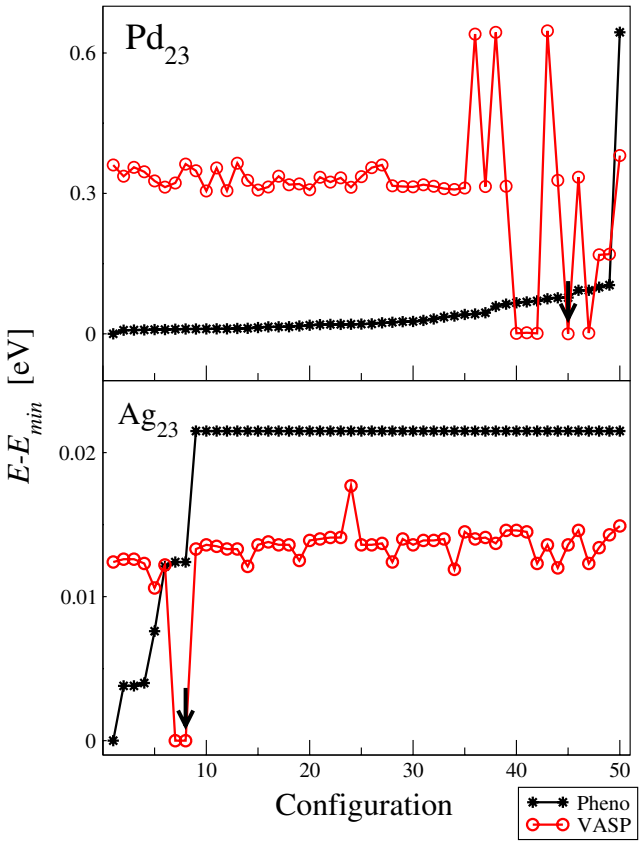

Figure 6. Energies of 23 atom clusters of palladium and silver, computed both with phenomenological potentials (stars) and after relaxation with VASP (open circles); the lines are just a guide to the eye. All energy values are referred to the minimum energy configuration. The arrows denote the specimens that attain the energy minimum after VASP relaxation.

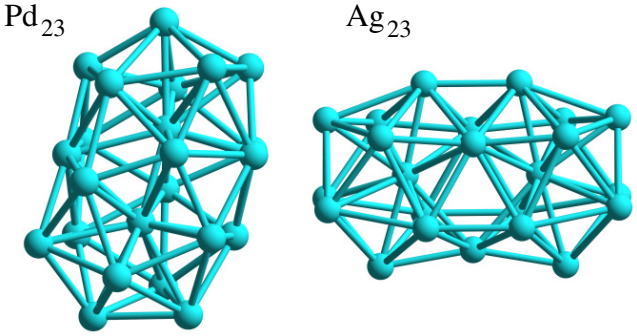

Figure 7. Geometric configuration of the 23 atom palladium and silver clusters with lowest energies as obtained with our procedure.

Table 2. Several physical properties of our lowest energy clusters. E_{coh}: cohesive energy per atom, in eV; d: average nearest neighbors distance, in Å units; r_c: cutoff radius for nearest neighbor distance, in Å units; SG: symmetry group, FBC: fraction of cluster atoms with bulk coordination, AC: average coordination, μ: magnetic moment, in Bohr magnetons.

Cluster	E_{coh} (eV)	d (Å)	r_c (Å)	SG	FBC	AC	μ (μ_B)
Rh_5	2.91	2.50	2.7	D_{3h}	—	3.6	3.0
Pd_5	1.78	2.64	2.9	D_{3h}	—	3.6	2.0
Ag_5	1.28	2.73	2.9	C_2	—	2.8	1.0
Pt_5	2.85	2.48	2.7	C_2	—	2.4	0.5
Au_5	1.76	2.68	2.9	C_s	0	2.8	0.6
Rh_{13}	3.79	2.59	3.2	C_{3v}	0	5.5	11.0
Pd_{13}	2.29	2.71	3.2	C_s	0	5.8	6.0
Ag_{13}	1.68	2.85	3.2	C_2	0	5.7	1.0
Pd_{23}	2.58	2.73	3.2	C_s	1/23	6.8	0.0
Ag_{23}	1.83	2.89	3.2	C_s	2/23	7.0	1.0

as much diversity as feasible, since prejudiced choices, based on the ideas that: (i) the minimum energy configuration obtained via phenomenological potentials does coincide with the one computed after DFT refinement; or, (ii) high symmetry structures are the most stable ones, are not supported by extensive computations [27, 61, 56].

Thus, we have implemented a diversity driven unbiased search scheme (DDUS), which starts with the creation of a diverse data bank of configurations that were minimized using phenomenological potentials. This algorithm is based on the conformational space annealing method (CSA) mentioned above. Next, *all* the elements in the bank are refined via DFT in order to obtain putative minima. This way, we are able to obtain not only the lowest energy configuration, but a set of low lying ones that often differ only slightly in energy. Since experiments are not carried out at absolute zero it is most likely that they generate a mixed set of low energy configurations. Moreover, at finite temperatures one expects this set to be stable.

An interesting illustration of the above is the structure of Pd_{13}. Previously [56], using the GA and relaxing with the SIESTA code, we found the icosahedron as the lowest energy configuration. Using DDUS with VASP refinement

we obtain several structures with lower energies than the Pd_{13} icosahedron, but the energy reduction only amounts to ≈0.25 eV.

We have applied our scheme to rhodium, palladium, silver, platinum and gold clusters of 5, 13 and 23 atoms. The results stress the fact that prejudiced choices of putative minima are risky to make. In addition, we have been able to obtain several novel minima for the above mentioned cluster structures. Of particular interest are the planar minimal configurations of Ag_5, Pt_5 and Au_5.

The main idea we want to convey is that an unbiased search improves the probability of obtaining the global minimum configuration. To prove our point we have implemented a scheme that, starting with the generation of a data bank of putative minima, allows for an unbiased search of minimum energy configurations of small clusters. As a result of its implementation it becomes quite apparent that a biased search, on a set of high symmetry configurations or simple refinement of minimum configurations obtained via phenomenological potentials, is not sufficient. In contrast, a full DFT relaxation of a relatively large and diverse data bank does improve the probability of obtaining global minima. It also allows one to find a set of low lying configurations which could prove useful in interpreting finite temperature experimental data.

Acknowledgments

This work was supported by the *Fondo Nacional de Investigaciones Científicas y Tecnológicas* (FONDECYT, Chile) under grants Nos 1070080 and 1071062 (JR and MK), No. 1080239 (RR and GG), Nos 1060830 and 1080658 (VM) and No. 1070854 (JAV). MR was supported by the *Comisión Nacional de Ciencia y Tecnología* (CONICyT, Chile).

References

[1] Bansmann J, Baker S H, Binns C, Blackman J A, Bucher J P, Dorantes-Davila J, Dupuis V, Favre L, Kechrakos D, Kleibert A, Meiwes-Broer K H, Pastor G M, Perez A, Toulemonde O, Trohidou K N, Tuaillon J and Xie Y 2005 *Surf. Sci. Rep.* **56** 189 and references therein
[2] Goedecker S, Hellmann W and Lenosky T 2005 *Phys. Rev. Lett.* **95** 055501
[3] Wales D J and Doye J P K 1997 *J. Phys. Chem.* **101** 5111
[4] Juhás P, Duxbury P M, Punch W F and Billinge S L 2006 *Nature* **440** 655 and references therein
[5] Joswig J O and Springborg M 2003 *Phys. Rev.* B **68** 085408
[6] Grigoryan V G and Springborg M 2003 *Chem. Phys. Lett.* **375** 219
[7] Grigoryan V G and Springborg M 2004 *Phys. Rev.* B **70** 205415
[8] Grigoryan V G, Alamova D and Springborg M 2006 *Phys. Rev.* B **73** 115415
[9] Dong Y and Springborg M 2007 *J. Phys. Chem.* C **111** 12528
[10] Doye J P K 2005 *Global Optimization–Selected Case Studies* ed J D Pinter Kluwer at press [arXiv:cond-mat/000738v2]
[11] Springborg M 2006 *Determination of Structure in Electronic Structure Calculations* vol 4 (Cambridge: Royal Society of Chemistry) chapter 6, pp 249–323 and references therein
[12] Daw M S and Baskes M I 1984 *Phys. Rev.* B **29** 6443
[13] Finnis M W and Sinclair J E 1984 *Phil. Mag.* A **50** 45
[14] Gupta R P 1985 *Phys. Rev.* B **23** 6265
[15] Baletto F, Mottet C and Ferrando R 2003 *Phys. Rev. Lett.* **90** 135504
[16] Baletto F and Ferrando R 2005 *Rev. Mod. Phys.* **77** 371 and references therein
[17] Guirado-López R, Desjonquérs M C and Sapnjaard D 2000 *Phys. Rev.* B **62** 13188
[18] Barreteau C, Guirardo-López R, Desjonquèrs M C and Oleś A M 2000 *Phys. Rev.* B **61** 7781
[19] Aguilera-Granja F, Bouarab S, Lopez M J, Vega A, Montejano-Carrizales J M, Iñiguez M P and Alonso J A 1998 *Phys. Rev.* B **57** 12469
[20] Hernández-Torres J, Aguilera-Granja F and Vega A 2001 *Solid State Commun.* **117** 477
[21] Aguilera-Granja F, Rodríguez-López J L, Michaelian K, Berlanga-Ramírez E O and Vega A 2002 *Phys. Rev.* B **66** 224410
[22] Yang M L, Jackson K A, Koehler C, Frauenheim T and Jellinek J 2006 *J. Chem. Phys.* **124** 024308
[23] Yang M L, Jackson K A and Jellinek J 2006 *J. Chem. Phys.* **125** 144308
[24] Chang C M and Chou M Y 2004 *Phys. Rev. Lett.* **93** 133401
[25] Hartke B 1999 *J. Comput. Chem.* **20** 1752
[26] Rossi G and Ferrando R 2006 *Chem. Phys. Lett.* **423** 17
[27] Rogan J, García G, Loyola C, Orellana W, Ramírez R and Kiwi M 2006 *J. Chem. Phys.* **125** 214708
[28] Lee J, Scheraga H A and Rackovsky S 1997 *J. Comput. Chem.* **18** 1222
[29] Lee J, Scheraga H A and Rackovsky S 1998 *Biopolymers* **46** 103
[30] Lee J, Scheraga H A and Rackovsky S 1999 *Int. J. Quantum Chem.* **75** 255
[31] Rossi G, Rapallo A, Mottet C, Fortunelli A, Baletto F and Ferrando R 2006 *Phys. Rev. Lett.* **93** 105503
[32] Paz-Borbón L O, Johnston R L, Barcarao G and Fortunelli A 2007 *J. Phys. Chem.* C **111** 2936
[33] Alcántara-Ortigoza M A and Rahman T 2008 *Phys. Rev.* B **77** 195404
[34] Lee J, Lee I-H and Lee J 2003 *Phys. Rev. Lett.* **91** 080201
[35] Byrd R H, Lu P, Nocedal J and Zhu C 1995 *SIAM J. Sci. Comput.* **16** 1190
[36] Cleri F and Rosato V 1993 *Phys. Rev.* B **48** 22
[37] Ferrando R, Fortunelli A and Johnston R L 2008 *Phys. Chem. Chem. Phys.* **10** 640
[38] Foiles S M, Baskes M I and Daw M S 1986 *Phys. Rev.* B **33** 7983
[39] Voter A F and Chen S P 1987 Characterization of defects in materials *MRS Symposia Proceedings* vol 82, ed R W Siegal, J R Weertman and R Sinclair (Washington, DC: Materials Research Society) p 175
[40] Ducastelle F 1970 *J. Physique* **31** 1055
[41] Sutton A P and Chen J 1990 *Phil. Mag. Lett.* **61** 139
[42] Murrell J N and Mottram R E 1990 *Mol. Phys.* **69** 571
[43] Cox H, Johnston R L and Murrell J N 1990 *J. Solid State Chem.* **145** 571
[44] Grigoryan V G, Alamanova D and Springborg M 2005 *Eur. Phys. J.* D **34** 187
[45] Deaven D M, Tit N, Morris J R and Ho K M 1996 *Chem. Phys. Lett.* **256** 195
[46] Mitchell M 1998 *An Introduction to Genetic Algorithms* (Cambridge, MA: MIT Press)
[47] Michaelian K, Rendón N and Garzón I L 1999 *Phys. Rev.* B **60** 2000
[48] Johnston R L 2003 *J. Chem. Soc. Dalton Trans.* (22) 4193
[49] Sebetci A and Güvenç Z B 2004 *Eur. Phys. J.* D **30** 71
[50] Kresse G and Hafner J 1993 *Phys. Rev.* B **47** 558
[51] Kresse G and Furthmüller J 1996 *Comput. Mater. Sci.* **6** 15
[52] Kresse G and Furthmüller J 1996 *Phys. Rev.* B **54** 11169
[53] Kresse G and Joubert D 1999 *Phys. Rev.* B **59** 1758
[54] Kresse G and Hafner J 1994 *J. Phys.: Condens. Matter* **6** 8245

[55] Perdew J P and Wang Y 1992 *Phys. Rev.* B **45** 13244
[56] Rogan J, García G, Valdivia J A, Orellana W, Romero A H, Ramírez R and Kiwi M 2005 *Phys. Rev.* B **72** 115421
[57] Rogan J, García G, Ramírez M, Muñoz V, Valdivia J A, Andrade X, Ramírez R and Kiwi M 2008 *Nanotechnology* **19** 205701
[58] Bae Y-C, Asani H, Kumar V and Kawazoe Y 2004 *Phys. Rev.* B **70** 195413
[59] Wang L-L and Johnson D D 2007 *Phys. Rev.* B **75** 235405
[60] Futschek T, Marsman M and Hafner J 2005 *J. Phys.: Condens. Matter* **17** 5927
[61] Kumar V and Kawazoe Y 2002 *Phys. Rev.* B **66** 144413